

Isoscalar giant monopole resonance and its overtone in microscopic and macroscopic models

S. Shlomo¹⁾, V. M. Kolomietz^{1,2)} and B.K. Agrawal¹⁾

¹⁾*Cyclotron Institute, Texas A&M University,
College Station, Texas 77843, USA*

²⁾*Institute for Nuclear Research, Kiev 03680, Ukraine*

Abstract

We calculate the transition density for the overtone of the isoscalar giant monopole resonance (ISGMR) from the response to an appropriate external field $\sim \hat{f}_\xi(\mathbf{r})$ obtained using the semiclassical fluid dynamic approximation and the Hartree-Fock (HF) based random phase approximation (RPA). We determine the mixing parameter ξ by maximizing the ratio of the energy-weighted sum for the overtone mode to the total energy-weighted sum rule and derive a simple expression for the macroscopic transition density associated with the overtone mode. This macroscopic transition density agrees well with that obtained from the HF-RPA calculations. We also point out that the ISGMR and its overtone can be clearly identified by considering the response to the electromagnetic external field $\sim j_0(qr)$.

PACS numbers: PACS numbers : 21.60.Jz, 24.30.Cz, 26.60.Ev, 24.10.Nz

I. INTRODUCTION

The properties of a giant resonance in nuclei are commonly determined from the distorted wave Born approximation (DWBA) analysis of its excitation cross-section by inelastic scattering of a certain projectile. The transition potential required in actual implementation of DWBA calculation is usually obtained by convoluting the projectile-nucleus interaction with the transition density associated with the giant resonance. The relevant transition density can be obtained from a microscopic theory of the giant resonance, such as the Hartree-Fock (HF) based random phase approximation (RPA). However, the use of a macroscopic transition density $\rho_{\text{tr}}^{\text{macr}}(\mathbf{r})$ greatly simplifies the application of the giant multipole resonance theory to the analysis of the experimental data. The simple form of the transition density

$$\rho_{\text{tr}}^{\text{sc}}(\mathbf{r}) = \alpha_0 \left(3 + r \frac{d}{dr} \right) \rho_{\text{eq}}(r) Y_{00}(\hat{\mathbf{r}}), \quad (1)$$

obtained by the scaling approximation, is a well-known example of the macroscopic transition density $\rho_{\text{tr}}^{\text{macr}}(\mathbf{r})$ commonly used in the case of the isoscalar giant monopole resonance (ISGMR) [1]. The transition density of Eq. (1) nicely agrees with the ISGMR transition density obtained in microscopic HF-RPA calculations. It has a one-node structure, satisfying the condition of particle number conservation $\int \rho_{\text{tr}}^{\text{sc}}(\mathbf{r}) d\mathbf{r} = 0$. Unfortunately the scaling consideration can not be extended to the overtone of the ISGMR, where $\rho_{\text{tr}}^{\text{macr}}(\mathbf{r})$ has a two-node structure. To derive the macroscopic transition density $\rho_{\text{tr}}^{\text{macr}}(\mathbf{r})$ in this more general case, one can use the well-known method [2, 3] of determining $\rho_{\text{tr}}^{\text{macr}}(\mathbf{r})$ from the local sum rule which is exhausted by one collective state with the appropriate choice of the transition operator $\hat{f}_{\xi}(\mathbf{r})$. However, in the quantum random phase approximation, the highly excited collective modes are strongly fragmented over a wide range of energy and a special averaging procedure must be employed to determine the macroscopic transition density corresponding to an average collective excitation. In this respect, the semiclassical Fermi-liquid approach (FLA) [4] is more appropriate. Both the main ISGMR and its overtone are well-defined within the FLA as single resonance states. This fact enables us to derive the transition operator $\hat{f}_{\xi}(\mathbf{r})$ simply by maximizing the fraction of the energy-weighted sum rule (FEWSR) exhausted by the single overtone.

In the present work we suggest a procedure to derive the macroscopic transition density for the ISGMR overtone using both the HF based RPA and the Fermi-liquid approaches.

We remark that some preliminary results of this investigation were presented in Ref. [5] (see also Ref. [6]).

II. QUANTUM DERIVATIONS

The transition density $\rho_{\text{tr},n}(\mathbf{r})$ for a certain eigenstate $|n\rangle$ of a nucleus with A nucleons is given by

$$\rho_{\text{tr},n}(\mathbf{r}) = \langle 0 | \hat{\rho}(\mathbf{r}) | n \rangle, \quad (2)$$

where $\hat{\rho}(\mathbf{r}) = \sum_{i=1}^A \delta(\mathbf{r} - \mathbf{r}_i)$ is the particle density operator and $|0\rangle$ represents the ground state of the nucleus. The transition density reflects the internal structure of the nucleus and does not depend on the external field. However, a problem arises if one intends to derive the transition density $\rho_{\text{tr}}(\mathbf{r})$ for a group of the thin-structure resonances in the giant multipole resonance (GMR) region. An appropriate averaging procedure is necessary in this case and $\rho_{\text{tr}}(\mathbf{r})$ can be evaluated if the nucleus is placed in an external field

$$V_{\text{ext}} \sim \hat{F}(\{\mathbf{r}_i\}) = \sum_{i=1}^A \hat{f}(\mathbf{r}_i), \quad (3)$$

where the transition operator $\hat{F}(\{\mathbf{r}_i\})$ is so chosen that it provides a preferable excitation of the above mentioned thin-structure resonances.

Let us introduce the local strength function

$$S(\mathbf{r}, E) = \sum_n \langle 0 | \hat{\rho}(\mathbf{r}) | n \rangle \langle n | \hat{F} | 0 \rangle \delta(E - E_n) \quad (4)$$

and the energy smeared local strength function $\tilde{S}(\mathbf{r}, E)$ defined near the GMR energy E_R by

$$\tilde{S}(\mathbf{r}, E_R) = \frac{1}{\Delta E} \int_{E_R - \Delta E/2}^{E_R + \Delta E/2} dE S(\mathbf{r}, E). \quad (5)$$

The corresponding strength functions are given by

$$S(E) = \int d\mathbf{r} \hat{f}(\mathbf{r}) S(\mathbf{r}, E) = \sum_n \left| \int d\mathbf{r} \hat{f}(\mathbf{r}) \rho_{\text{tr},n}(\mathbf{r}) \right|^2 \delta(E - E_n), \quad (6)$$

and

$$\tilde{S}(E) = \int d\mathbf{r} \hat{f}(\mathbf{r}) \tilde{S}(\mathbf{r}, E). \quad (7)$$

Let us assume, for the moment, that the operator $\hat{F}(\{\mathbf{r}_i\})$ excites only a single state $|D\rangle$, within the energy interval $E_R \pm \Delta E/2$. The corresponding transition density $\rho_{\text{tr},D}(\mathbf{r}) = \langle 0|\hat{\rho}(\mathbf{r})|D\rangle$ is then given by the following *exact* expression

$$\rho_{\text{tr},D}(\mathbf{r}) = \frac{\Delta E}{\sqrt{\tilde{S}(E_R) \Delta E}} \tilde{S}(\mathbf{r}, E_R). \quad (8)$$

We will extend expression (8) to the case of a group of the thin-structure resonances in the GMR region which are excited by the operator $\hat{F}(\{\mathbf{r}_i\})$ and define the smeared transition density $\tilde{\rho}_{\text{tr},R}(\mathbf{r})$ as

$$\tilde{\rho}_{\text{tr},R}(\mathbf{r}) = \frac{\Delta E}{\sqrt{\tilde{S}(E_R) \Delta E}} \tilde{S}(\mathbf{r}, E_R). \quad (9)$$

Note that Eq. (9) is associated with the strength in the region of $E_R \pm \Delta E/2$ and is consistent with the smeared strength function $\tilde{S}(E_R)$ for a single resonance state. That is (see also Eq. (6)),

$$\tilde{S}(E_R) = \frac{1}{\Delta E} \left| \int d\mathbf{r} \hat{f}(\mathbf{r}) \tilde{\rho}_{\text{tr},R}(\mathbf{r}) \right|^2. \quad (10)$$

We also point out that with the Lorentz's function

$$g_\gamma(E, E_R) = \frac{1}{\pi} \frac{\gamma}{(E - E_R)^2 + \gamma^2}, \quad (11)$$

the energy smeared $\tilde{S}(\mathbf{r}, E_R)$ is given by

$$\tilde{S}(\mathbf{r}, E_R) = \int_{-\infty}^{\infty} dE S(\mathbf{r}, E) g_\gamma(E, E_R), \quad (12)$$

and the smeared transition density $\tilde{\rho}_{\text{tr},R}(\mathbf{r})$ is obtained from

$$\tilde{\rho}_{\text{tr},R}(\mathbf{r}) = \frac{\pi\gamma}{\sqrt{\tilde{S}(E_R) \pi\gamma}} \tilde{S}(\mathbf{r}, E_R). \quad (13)$$

The consistency condition, Eq. (10), then reads

$$\tilde{S}(E_R) = \frac{1}{\pi\gamma} \left| \int d\mathbf{r} \hat{f}(\mathbf{r}) \tilde{\rho}_{\text{tr},R}(\mathbf{r}) \right|^2. \quad (14)$$

In the quantum RPA, the local strength function $S(\mathbf{r}, E)$ is related to the RPA Green's function $G(\mathbf{r}', \mathbf{r}, E)$ by [7, 8]

$$S(\mathbf{r}, E) = \int d\mathbf{r}' \hat{f}(\mathbf{r}') \left[\frac{1}{\pi} \text{Im} G(\mathbf{r}', \mathbf{r}, E) \right] d\mathbf{r}'. \quad (15)$$

For the isoscalar monopole and dipole excitations, the transition operator $\hat{f}(\mathbf{r})$ is taken in the form of

$$\hat{f}(\mathbf{r}) \equiv \hat{f}_\xi(\mathbf{r}) = f_\xi(r)Y_{00}(\hat{\mathbf{r}}) \quad \text{for } L = 0, \quad (16)$$

and

$$\hat{f}(\mathbf{r}) \equiv \hat{f}_\eta(\mathbf{r}) = f_\eta(r)Y_{10}(\hat{\mathbf{r}}) \quad \text{for } L = 1, \quad (17)$$

with an appropriate choice of the radial functions $f_\xi(r)$ and $f_\eta(r)$, see below. In the following, the quantum transition density for the main ISGMR and its overtone is evaluated using the Eq. (9) with $E_R \pm \Delta E/2$ taken separately for the ISGMR and the overtone regions.

III. MACROSCOPIC TRANSITION DENSITY

Let us consider the local energy-weighted sum $M_1(\mathbf{r})$ given by (see Eq. (4))

$$M_1(\mathbf{r}) = \int_0^\infty dE ES(\mathbf{r}, E) = \sum_n E_n \langle 0|\hat{\rho}(\mathbf{r})|n\rangle \langle n|\hat{F}|0\rangle, \quad (E_0 = 0). \quad (18)$$

The continuity equation provides the following sum rule [3]

$$M_1(\mathbf{r}) = -\frac{\hbar^2}{2m} \left(\rho_{\text{eq}} \nabla \hat{f}(\mathbf{r}) \right). \quad (19)$$

Let us assume that only one state $|D\rangle$ exhausts the sum rule Eq. (19). Then for the corresponding ("macroscopic") transition density, $\rho_{\text{tr}}^{\text{macr}}(\mathbf{r})$, we have from Eqs. (18) and (19) the following expression

$$\rho_{\text{tr}}^{\text{macr}}(\mathbf{r}) = \langle 0|\hat{\rho}(\mathbf{r})|D\rangle = \alpha_0 \nabla \left(\rho_{\text{eq}} \nabla \hat{f}(\mathbf{r}) \right), \quad (20)$$

where the normalization coefficient α_0 can be found using the energy-weighted sum rule (EWSR)

$$m_1 = \int d\mathbf{r} \hat{f}(\mathbf{r}) M_1(\mathbf{r}) = \frac{\hbar^2}{2m} \int d\mathbf{r} \rho_{\text{eq}} \left(\nabla \hat{f}(\mathbf{r}) \right)^2. \quad (21)$$

Taking into account that

$$\langle D|\hat{F}|0\rangle = \left(\int d\mathbf{r} \hat{f}(\mathbf{r}) \rho_{\text{tr}}^{\text{macr}}(\mathbf{r}) \right)^*,$$

we obtain

$$|\alpha_0| = (\hbar^2/2m)(E_D m_1)^{-1/2}. \quad (22)$$

Thus, the macroscopic transition density $\rho_{\text{tr}}^{\text{macr}}(\mathbf{r})$ of Eq. (20) coincides with the quantum transition density for a certain state $|D\rangle$ if the single state $|D\rangle$ exhausts all the EWSR, Eq. (21), associated with the transition operator $\hat{f}(\mathbf{r})$. In the case of the transition operator $\hat{f}(\mathbf{r})$ from Eqs. (16) and (17), the EWSR is given by [2]

$$m_1 = \frac{\hbar^2}{2m} \frac{A}{4\pi} (2L+1) \left[\left\langle 0 \left| \left(\frac{df}{dr} \right)^2 + L(L+1) \left(\frac{f}{r} \right)^2 \right| 0 \right\rangle \right]. \quad (23)$$

Assuming that the energy-weighted transition strength (EWTS) $E_D |\langle D | \hat{F} | 0 \rangle|^2$ for the resonance at E_D fully exhausts the EWSR associated with $\hat{f}(\mathbf{r}) = f(r) Y_{LM}(\hat{\mathbf{r}})$, we obtain the expression for the macroscopic transition density for the state at E_D from Eq. (20) [9]

$$\rho_{\text{tr}}^{\text{macr}}(\mathbf{r}) = -\frac{\hbar^2}{2m} \sqrt{\frac{2L+1}{m_1 E_D}} \left[\frac{1}{r} \frac{d^2}{dr^2} (r f) - \frac{L(L+1)}{r^2} f + \frac{df}{dr} \frac{d}{dr} \right] \rho_{\text{eq}}(r) Y_{LM}(\hat{\mathbf{r}}). \quad (24)$$

For $L=0$ we have from Eq. (24) the commonly used ISGMR result of Eq. (1). The main (lowest) ISGDR is the spurious state with the eigenenergy $E_{1^-} = 0$. The next ISGDR is the overtone. Assuming that the EWTS for the 1^- overtone equals the EWSR associated with the operator

$$\hat{f}_\eta(\mathbf{r}) = (r^3 - \eta r) Y_{10}(\hat{\mathbf{r}}), \quad (25)$$

we obtain from Eq. (20) the macroscopic transition density as

$$\rho_{\text{tr, overtone}}^{\text{macr}}(\mathbf{r}) = \alpha_0 \sqrt{3} \left(10 r + (3 r^2 - \eta) \frac{d}{dr} \right) \rho_{\text{eq}}(r) Y_{10}(\hat{\mathbf{r}}) \quad \text{for} \quad L=1. \quad (26)$$

For the isoscalar dipole mode, the translation invariance condition is used for the derivation of η . This condition implies that the center of mass of the system can not be affected by internal excitation. We thus have,

$$\int d\mathbf{r} r Y_{10}^*(\hat{\mathbf{r}}) \rho_{\text{tr}}^{\text{macr}}(\mathbf{r}) = 0 \quad \text{for} \quad L=1. \quad (27)$$

From Eqs. (26) and (27) one obtains, see also Refs. [10, 11, 12],

$$\eta = \frac{5}{3} \langle r^2 \rangle, \quad (28)$$

where $\langle r^2 \rangle = \int_0^\infty dr r^4 \rho_{\text{eq}}(r) / \int_0^\infty dr r^2 \rho_{\text{eq}}(r)$ is the mean square radius.

The free (mixing) parameter appearing in the transition operator $\hat{f}_\xi(\mathbf{r})$ (similar to η of Eq. (17) for the $L=1$ case) can be determined by an appropriate condition leading to a general method for the evaluation of the transition density for the overtone mode. In this

work we present this method for the case of the monopole mode, $L = 0$. Let us introduce the transition operator $\hat{f}_\xi(\mathbf{r})$ as

$$\hat{f}_\xi(\mathbf{r}) = (r^4 - \xi r^2)Y_{00}(\hat{\mathbf{r}}) \quad \text{for } L = 0. \quad (29)$$

The corresponding macroscopic transition density $\rho_{\text{tr}}^{\text{macr}}(\mathbf{r})$ is obtained from Eqs. (20) and (29) as

$$\rho_{\text{tr}}^{\text{macr}}(\mathbf{r}) = 2\alpha_0 \left[10r^2 - 3\xi + r(2r^2 - \xi) \frac{d}{dr} \right] \rho_{\text{eq}}(r)Y_{00}(\hat{\mathbf{r}}) \quad \text{for } L = 0 \quad (\text{overtone}). \quad (30)$$

The determination of the parameter ξ in Eq. (30) requires an additional consideration since for the $L = 0$ case we have no fundamental condition such as Eq. (27) for the $L = 1$ mode. We note, however, that if we assume that the ISGMR has the transition density of Eq. (1) and require that

$$\int d\mathbf{r} \hat{f}_\xi(\mathbf{r}) \rho_{\text{tr}}^{\text{sc}}(\mathbf{r}) = 0, \quad (31)$$

i.e., the ISGMR is not excited by the scattering operator of Eq. (29) we have

$$\xi = 2\langle r^4 \rangle / \langle r^2 \rangle. \quad (32)$$

Similar result is obtained by imposing the condition that the scattering operator $r^2 Y_{00}(\hat{\mathbf{r}})$ does not excite the overtone of the ISGMR, assuming the transition density of Eq. (30).

Following the general requirement for the proper use of Eq. (20) in the derivation of the macroscopic transition density $\rho_{\text{tr}}^{\text{macr}}(\mathbf{r})$, we can determine the parameter ξ from the condition that the transition operator $\hat{f}_\xi(\mathbf{r})$ provides for the single overtone the maximum fraction of the energy-weighted sum rule m_1 of Eq. (21).

IV. SEMICLASSICAL FERMI-LIQUID APPROACH

The transition density $\rho_{\text{tr}}(\mathbf{r})$ and the strength function $S(E)$ can also be evaluated within the semiclassical Fermi-liquid approach. For a given multipolarity L and overtone n , the FLA transition density is given by [4]

$$\rho_{\text{tr},Ln}^{\text{FLA}}(\mathbf{r}) = \alpha_{Ln} [\theta(R_0 - r)j_L(q_{Ln}r) +$$

$$\left. \frac{1-a}{q_{Ln}} \delta_{L1} \delta(R_0 - r) j_L'(q_{Ln} R_0) \right] \rho_0 Y_{L0}(\hat{\mathbf{r}}), \quad (33)$$

where ρ_0 is the bulk density, R_0 is the equilibrium nuclear radius and the parameter a is determined by the translation invariance condition (Eq. (27)) in the case of the isoscalar dipole compression mode and is given by

$$a = j_1(x)/x j_1'(x), \quad x = q_{Ln} R_0. \quad (34)$$

The wave numbers q_{Ln} are derived from the boundary conditions of the FLA model: the normal component of the tensor pressure $\delta P_{\nu\mu}$, created by a sound wave, on the free surface of the nucleus should be equal to zero

$$\delta P_{rr}|_{R=R_0} = 0. \quad (35)$$

Note that for the case of compression sound modes, the contribution from the surface tension pressure is negligible and it was omitted in Eq. (35). The boundary condition (Eq. (35)) leads to the following secular equation (see Ref. [15])

$$[qr j_0(qr) - D_\mu j_1(qr)]_{r=R_0} = 0, \quad D_\mu = \frac{4\mu}{m \rho_0 c_0^2}, \quad (36)$$

where c_0 is the zero sound velocity and the coefficient μ determines the contribution from the dynamical Fermi surface distortion associated with the collective motion in a Fermi liquid. In the case of a quadrupole distortion of the Fermi surface, one has [16]

$$\mu = \text{Im} \left(\frac{\omega\tau}{1 - i\omega\tau} \right) P_{\text{eq}}. \quad (37)$$

Here, $P_{\text{eq}} \approx (2/5)\epsilon_F \rho_0$ is the equilibrium pressure of a Fermi gas, ϵ_F is the Fermi energy, and ω and τ are the eigenfrequency and the relaxation time for sound excitations in the Fermi liquid, respectively. The relaxation time τ is assumed to be frequency dependent because of the memory effect in the collision integral [17]. Following Refs. [16, 18, 19] we take

$$\tau = 4\pi^2 \beta \hbar / (\hbar\omega)^2, \quad (38)$$

where β is the constant related to the differential cross section for the scattering of two nucleons in the nuclear interior. In the case of isoscalar sound mode, we will adopt $\beta = 1.5$ MeV [20]. The eigenfrequency ω is obtained from the dispersion relation

$$\omega^2 - c_0^2 q^2 + i\omega\gamma q^2 = 0, \quad (39)$$

where c_0 is given by

$$c_0^2 = \frac{1}{9m}(K + 12\mu/\rho_0). \quad (40)$$

Here K is the nuclear incompressibility coefficient and γ is the friction coefficient

$$\gamma = \frac{4\nu}{3\rho_0 m}, \quad \nu = \text{Re} \left(\frac{\tau}{1 - i\omega\tau} \right) P_{\text{eq}}. \quad (41)$$

The smeared FLA strength function $\tilde{S}^{\text{FLA}}(E)$ can be obtained in a way similar to $\tilde{S}(E)$, obtained within the quantum approach of Eq. (14). That is,

$$\tilde{S}^{\text{FLA}}(E) = \sum_n \left| \int d\mathbf{r} \rho_{\text{tr},Ln}^{\text{FLA}}(\mathbf{r}) \hat{f}(\mathbf{r}) \right|^2 g_\gamma(E, E_{Ln}). \quad (42)$$

The smearing function $g_\gamma(E, E_{Ln})$ in Eq. (42) is given by ($\gamma_{Ln} \ll E_{Ln}$)

$$g_\gamma(E, E_{Ln}) = \frac{1}{\pi} \frac{\gamma_{Ln}}{(E - E_{Ln})^2 + \gamma_{Ln}^2}, \quad \gamma_{Ln} = \frac{1}{2} \frac{\gamma}{\hbar} \frac{E_{Ln}^2}{c_0^2}. \quad (43)$$

Here, γ_{Ln} is the damping parameter due to the viscosity of the Fermi liquid and $E_{Ln} = \hbar \text{Re}(\omega_{Ln})$, where the eigenfrequency ω_n is obtained as a solution to both the dispersion equation (39) and the secular equation (36). We point out that the amplitude α_{Ln} in Eq. (33) for the FLA transition density $\rho_{\text{tr},Ln}^{\text{FLA}}(\mathbf{r})$ is derived as the amplitude of the quantum oscillations

$$\alpha_{Ln} = \sqrt{\hbar/2B_L(q) \omega(q)}, \quad (44)$$

where $q = q_{Ln}$ is determined by Eq. (36) and $B_L(q)$ is the corresponding mass coefficient with respect to the density oscillations. The collective mass coefficient $B_L(q)$ can be found from the collective kinetic energy E_{kin} for the particle density oscillations. The collective kinetic energy is derived as

$$E_{\text{kin}} = \frac{1}{2} m \rho_0 \int d\mathbf{r} v^2 = \frac{1}{2} B_L \dot{\alpha}_L^2. \quad (45)$$

For the compression modes $L = 0$, the mass coefficient B_0 is given by [4]

$$B_0 \equiv B_0(q) = (1/2)m \rho_0 R_0^5 x_0^{-4} [1 - j_0^2(x) - D_\mu j_1^2(x)]_{x=x_0}, \quad \text{for } L = 0, \quad (46)$$

where $x_0 = qR_0$.

V. RESULTS AND DISCUSSIONS

We have carried out calculations for the ISGMR in the frameworks of HF based RPA and the semiclassical Fermi liquid approach as briefly outlined in the preceding sections. We have evaluated the smeared FLA strength function $\tilde{S}^{\text{FLA}}(E)$ of Eq. (42) and the HF-RPA smeared strength function $\tilde{S}(E)$ of Eq. (14) for the ISGMR in several nuclei, for $\hat{f}_\xi(\mathbf{r})$ from Eq. (29). In the subsequent discussions, the HF-RPA results presented are obtained using the Skyrme force SkM* [21]. For the RPA calculations to be highly accurate we discretized the continuum in a large box of size 90 fm and use a smearing parameter $\gamma = \Gamma/2 = 1.0$ MeV, in evaluating the RPA Green's function (see Eq. (15)), and allow particle-hole excitations up to 500 MeV (see Ref. [9] for the details). In case of the FLA calculations we have adopted the values of $\rho_0 = 0.14 \text{ fm}^{-3}$, $\epsilon_F = 32.85$ MeV and $R_0 = 1.2 \cdot A^{1/3}$ fm. In Table I we compare the FLA and RPA results for the centroid energies E_{01} and E_{02} corresponding to the main and overtone mode of the ISGMR, respectively. We see from this table that the FLA and RPA results are in qualitative agreement. The small differences ($< 10\%$) can be understood by the fact that the centroid energy mainly depends on the size of the system. The values of the mean square radii and the higher moments of the ground state density distribution are smaller in the FLA than the ones obtained from HF calculations. Note also that the ratio E_{02}/E_{01} in both models considered is greater than two ($\sim 2.2 - 2.4$). We point out that $E_{02} > 2E_{01}$ is due to the Fermi-surface distortion effect as noted earlier in Ref. [15].

We have performed a comparison of the macroscopic transition density $\rho_{\text{tr}}^{\text{macr}}(\mathbf{r})$ with the ones obtained within the HF-RPA, $\rho_{\text{tr}}^{\text{HF-RPA}}(\mathbf{r})$, and the FLA, $\rho_{\text{tr}}^{\text{FLA}}(\mathbf{r})$, approaches for the main resonance $L = 0$ and its overtone. The FLA transition density is given by Eq. (33) with the wave number q obtained from the secular equation (36). The contribution of the ISGMR overtone to the EWSR for the case of the transition operator $\hat{f}_\xi(\mathbf{r})$ is given by

$$m_{02}(\xi) = E_{02} \left| \int d\mathbf{r} \hat{f}_\xi(\mathbf{r}) \rho_{\text{tr},02}^{\text{FLA}}(\mathbf{r}) \right|^2, \quad (47)$$

where $E_{02} = \hbar\omega(q_{02})$. The eigenfrequency $\omega(q_{02})$ is obtained from the dispersion equation (39) and the wave number q_{02} is the second (overtone) solution to the secular equation (36).

The EWSR for the transition operator $\hat{f}_\xi(\mathbf{r})$ reads

$$m_1(\xi) = \frac{\hbar^2}{2m} \int d\mathbf{r} \rho_{\text{eq}} \left(\nabla \hat{f}_\xi(\mathbf{r}) \right)^2. \quad (48)$$

Now, we will determine the parameter ξ from the condition that the value of the ratio of the partial sum $m_{02}(\xi)$ to the total sum $m_1(\xi)$ is the maximum. In Fig. 1, we have plotted the ratio $m_{02}(\xi)/m_1(\xi)$ as a function of the parameter ξ for the nucleus ^{208}Pb obtained in the FLA (dashed line) and the HF-RPA (solid line) models. As seen from Fig. 1, the maximum value of the ratio of $m_{02}(\xi)$ to $m_1(\xi)$ for the FLA model is achieved for $\xi = 68.3$ fm² where the overtone exhausts about 73% of the EWSR. In the case of HF-RPA, the maximum ratio is achieved for $\xi = 78.6$ fm² where the overtone, in the energy range of 25 - 50 MeV, exhausts about 60% of the EWSR. It is interesting to note that if we use the FLA and HF ground-state densities to calculate ξ from Eq. (32), we get $\xi = 72.2$ and 79.0 fm², respectively. These values are close to the corresponding ones (68.3 and 78.6 fm²) obtained by the condition of maximizing the ratio $m_{02}(\xi)/m_1(\xi)$. This means that the mixing parameter ξ in the transition operator $\hat{f}_\xi(\mathbf{r})$ of Eq. (29) can also be derived from the condition that the main ISGMR gives a minimal contribution to the energy-weighted sum rule $m_1(\xi)$. The FLA as well as HF-RPA calculations show that the difference in the values of ξ obtained in both conditions does not exceed $\sim 0.2\%$. We have also calculated the dependence of the parameter ξ on the nuclear mass number A . Following the same procedure we find for ^{90}Zr , ^{116}Sn and ^{144}Sm nuclei the value of mixing parameter $\xi = 38.6$ (48.5), 45.9 (56.7) and 53.1 (66.1) fm² from the FLA (RPA) calculations, respectively. These values can be well approximated by $\xi = 1.89A^{2/3}$ and $2.36A^{2/3}$ fm² for the FLA and RPA approaches, respectively.

In Fig. 2, we plot the FLA and RPA results for the fraction energy-weighted transition strength as a function of the excitation energy obtained for the transition operator $\hat{f}_\xi(\mathbf{r})$ for the ^{208}Pb nucleus. We use $\xi = 68.3$ and 78.6 fm² in the FLA and RPA calculations, respectively. One can clearly see that the RPA calculation yields a wide resonance of width of ~ 10 MeV around the excitation energy 30 – 35 MeV which corresponds to the ISGMR overtone. Whereas, in the case of FLA, the transition operator $\hat{f}_\xi(\mathbf{r})$ (Eq. (29)) with an appropriate value of ξ gives rise to a well defined resonance for the overtone mode. We also notice that the RPA results have the reminiscence of the ISGMR main tone but it is practically eliminated in the FLA calculations.

In Figs. 3a and 3b, we compare the radial macroscopic transition density $\rho_{\text{tr}}^{\text{macr}}(r)$ of Eq. (30), obtained using the HF ground-state density, and the corresponding FLA and HF-RPA ones for the overtone of the ISGMR. The radial transition density $\rho_{\text{tr}}(r)$ for a certain

multipolarity L is given by $\rho_{\text{tr}}(\mathbf{r}) = \rho_{\text{tr}}(r)Y_{L0}(\hat{\mathbf{r}})$. The macroscopic transition densities for the overtone in Figs. 3a and 3b are not the same. Because, for an appropriate comparison, in Fig. 3a, we have plotted $\rho_{\text{tr}}^{\text{macr}}(r)$ obtained using $\xi = 78.6 \text{ fm}^2$ and it is normalized to 60% of the EWSR. On the other hand, $\rho_{\text{tr}}^{\text{macr}}(r)$ plotted in Fig. 3b corresponds to $\xi = 68.3 \text{ fm}^2$ and is normalized to 73% of the EWSR. Further, the RPA transition density is calculated by averaging over the energy range of 25 - 50 MeV. Notice that the shift of the nodes of $\rho_{\text{tr},02}^{\text{FLA}}(r)$ to the left with respect to the ones of $\rho_{\text{tr}}^{\text{macr}}(r)$ is caused by the fact that in contrast to Eq. (30) used for the macroscopic transition density, in the FLA we use sharp nuclear surface, see Eq. (33). We also looked into the energy dependence of the RPA transition density for the operator $\hat{f}_{\xi}(\mathbf{r})$ over the range of energy employed for the averaging. We see that over the entire range considered, the transition density has two nodal structure and the distance between the nodes decreases with the increase in energy. For example, averaging over $\Delta E = 0.5 \text{ MeV}$ range, we find that at the excitation energies of 30, 40 and 50 MeV, the distances between the two nodes are 3.1, 2.7, and 2.4 fm, respectively, which reflects the fact that the microscopic transition density is state dependent.

We have used the microscopic transition densities for the operator $\hat{f}_{\xi}(\mathbf{r})$ to evaluate the cross-section for the ISGMR overtone mode excited via inelastic scattering of α -particles with energies 240 and 400 MeV. We have used the folding model (FM)-DWBA to calculate the excitation cross-section (see Ref. [23] for details). We find that for the α -particles with 400 MeV energy, the calculated cross-section is about 7 - 10 times higher than the one obtained for α -particles with 240 MeV. Note that for a monopole resonance the cross-section is maximum at 0° . The values of the cross-section at 0° for the peak energy of the ISGMR overtone are 0.5 and 3.5 mb/(sr MeV) for the case of 240 and 400 MeV, respectively. We point out that the maximum cross-section for the case of 240 MeV α -particles is below the current experimental sensitivity of about 2 mb/(sr MeV) [24]. It may be possible to identify the ISGMR overtone mode with 400 MeV α -particles.

The transition density $\rho_{\text{tr}}(\mathbf{r})$ for the compression modes is distributed over the nuclear interior and has a node close to the nuclear surface for both the main ISGMR and its overtone. The transition density $\rho_{\text{tr},02}(\mathbf{r})$ of the overtone has an additional node in the nuclear interior. This feature of $\rho_{\text{tr}}(\mathbf{r})$ can be tested by evaluating the strength distribution $S_0(k)$ of the electromagnetic operator $j_L(kr)Y_{L0}(\hat{r})$. The strength function $S_{0n}(k)$ for a

certain eigenstate n is given by

$$S_{0n}(k) = |I_{0n}(k)|^2 \quad (49)$$

where

$$I_{0n}(k) = \int d\mathbf{r} \rho_{\text{tr},0n}(\mathbf{r}) j_0(kr) Y_{00}(\hat{r}). \quad (50)$$

The strength function S_{0n} is related to the excitation function of electron-nucleus scattering in the Born approximation. We use Eqs. (49) and (50) to calculate the energy-weighted sums $m_{01}(k)$ and $m_{02}(k)$ for the main ISGMR and its overtone, respectively. In Fig. 4, we display the k dependence of the fraction energy-weighted sums $m_{01}(k)/m_1(k)$ and $m_{02}(k)/m_1(k)$ for the ^{208}Pb nucleus obtained from the FLA (dashed line) and HF-RPA (solid line) approaches. It can be seen from Fig. 4 that $m_{01}(k)/m_1(k)$ and $m_{02}(k)/m_1(k)$ depend strongly on k . A shift of the maximum of the ratio $m_{02}(k)/m_1(k)$ for the overtone to the higher value of wave number k is due to the more complicated nodal structure of the transition density associated with the overtone as compared with the main resonance. This shift can be exploited to separate the modes in electron-nucleus scattering. In Fig. 5 we plot the surface and the volume contributions to the integral in Eq. (50) for the transition density associated with overtone mode (see Eq. (33)). For smaller k , there is a cancellation between the surface and the volume contributions leading to a peak structure for the overtone response as shown in Fig. 4.

VI. SUMMARY AND CONCLUSIONS

Starting from the local strength function $S(\mathbf{r}, E)$ and using the smearing procedure, we have extended the quantum expression for the transition density $\rho_{\text{tr},n}(\mathbf{r})$ to the case of a group of the thin-structure resonances which are localized in the GMR region and are excited due to the specifically chosen transition operator $\hat{F}(\{\mathbf{r}_i\}) = \sum_{i=1}^A \hat{f}(\mathbf{r}_i)$. Our approach was applied to the study of the transition density of the ISGMR overtone. In this case, an appropriate form of the transition operator $\hat{f}(\mathbf{r})$ is given by $\hat{f}(\mathbf{r}) = \hat{f}_\xi(\mathbf{r}) = (r^4 - \xi r^2) Y_{00}(\hat{\mathbf{r}})$, see Eq. (29). The mixing parameter ξ was determined from the condition that the transition operator $\hat{f}_\xi(\mathbf{r})$ provides for the single overtone the maximum fraction of the energy-weighted sum rule m_1 of Eq. (21). The mixing parameter ξ depends on the nuclear mass number A . This dependence is well approximated by $\xi \approx 2 \cdot A^{2/3} \text{ fm}^2$.

We have applied our smearing procedure (using $\hat{f}_\xi(\mathbf{r})$ associated with the maximum FEWSR of the overtone) to the evaluation of the smeared out transition density $\tilde{\rho}_{\text{tr},\text{R}}(\mathbf{r})$ of Eq. (9) within the HF-RPA. We have shown that the smearing procedure for the ISGMR overtone region provides a simple two nodal structure of $\tilde{\rho}_{\text{tr},\text{R}}(\mathbf{r})$ (see the solid line in Fig. 3a), as expected for the $L = 0$ overtone. Moreover, the transition density $\tilde{\rho}_{\text{tr},\text{R}}(\mathbf{r})$, obtained by the averaging over many quantum states, resembles its macroscopic counterpart. This fact is well illustrated in Fig. 3a by comparing the quantum smeared transition density $\tilde{\rho}_{\text{tr},\text{R}}(\mathbf{r})$ with the macroscopic one $\rho_{\text{tr}}^{\text{macr}}(\mathbf{r})$ of Eq. (30). An independent derivation of the smeared out transition density $\tilde{\rho}_{\text{tr},\text{R}}(\mathbf{r})$ can be also obtained using the semiclassical approaches. In Sec. IV, we have applied a simple semiclassical Fermi-liquid approximation to the evaluation of the smeared out (in quantum mechanical sense) transition density $\rho_{\text{tr}}^{\text{FLA}}(\mathbf{r})$. We have used the same form of the transition operator $\hat{f}_\xi(\mathbf{r})$ as in the case of quantum HF-RPA calculation to provide an additional check of the derivation of the mixing parameter ξ from the energy-weighted sum m_1 . We found a good agreement between the values of parameter ξ obtained in both the quantum and the semiclassical approaches. It is important to emphasize that equation (32) together with Eq. (20) provides a simple expression for the macroscopic transition density that can be employed in the folding model-DWBA analysis of excitation cross-section of the ISGMR overtone.

The nodal structure of the semiclassical transition density $\rho_{\text{tr}}^{\text{FLA}}(\mathbf{r})$ is similar to that of both the quantum, $\tilde{\rho}_{\text{tr},\text{R}}(\mathbf{r})$, and the macroscopic, $\rho_{\text{tr}}^{\text{macr}}(\mathbf{r})$, cases, see Figs. 3a and 3b. A discrepancy occurs in the surface region, where the particular behavior of $\rho_{\text{tr}}^{\text{FLA}}(\mathbf{r})$ is due to the assumption of the sharp surface of the nucleus in the FLA model. This discrepancy is not so significant in the integral quantities like the strength functions. This is illustrated in Fig. 4 for the case of the nuclear response to the electromagnetic-like external field $\sim j_0(kr)Y_{00}(\hat{\mathbf{r}})$. The ratios $m_{01}(k)/m_1(k)$ and $m_{02}(k)/m_1(k)$ for the ISGMR and its overtone, respectively, show a distinct feature in the k -dependence. Namely, for a certain value of the wave number k , the strength function for the overtone reaches a maximum whereas the contribution of the main resonance to the strength function is strongly suppressed. This fact can be exploited to separate the ISGMR and the overtone modes in electron-nucleus scattering by varying the electron's momentum transfer k .

VII. ACKNOWLEDGMENTS

This work was supported in part by the US Department of Energy under grant # DOE-FG03-93ER40773. One of us (V.M.K.) thank the Cyclotron Institute at Texas A&M University for the kind hospitality.

-
- [1] J. P. Blaizot, Phys. Rep. **64**, 171 (1980).
 - [2] A. Bohr and B. Mottelson, *Nuclear Structure* (Benjamin, London, 1975), Vol. II, Ch. 6.
 - [3] P. Ring and P. Schuck, *The nuclear many-body problem* (Springer, New York-Heidelberg-Berlin, 1980).
 - [4] V.M. Kolomietz and S. Shlomo, Phys. Rev. C **61**, 064302 (2000).
 - [5] S. Shlomo, A. I. Sanzhur and V. M. Kolomietz, Progress in Research, (Cyclotron Institute, Texas A&M University, Texas, 2001), p. III-5.
 - [6] N. L. Gorlik and M. H. Urin, nucl-th/0209094v1.
 - [7] G.F. Bertsch and S.F. Tsai, Phys. Rep. **18**, 125 (1975).
 - [8] S. Shlomo and G.F. Bertsch, Nucl. Phys. **A243**, 507 (1975).
 - [9] B.K. Agrawal, S. Shlomo and A. I. Sanzhur, Phys. Rev. C **67**, 034314 (2003).
 - [10] I. Hamamoto, H. Sagawa and X.Z. Zhang, Phys. Rev. C **57**, R1064 (1998).
 - [11] M.H. Harakeh, Phys. Lett. **B90**, 13 (1980).
 - [12] T.J. Deal, Nucl. Phys. **A217**, 210 (1973).
 - [13] S. Shlomo and A. I. Sanzhur, Phys. Rev. C **65**, 044310 (2002).
 - [14] V.M. Kolomietz, S.V. Radionov and S. Shlomo, Phys. Rev. C **64**, 054302 (2001).
 - [15] A. Kolomiets, V.M. Kolomietz and S. Shlomo, Phys. Rev. C **59**, 3139 (1999).
 - [16] D. Kiderlen, V. M. Kolomietz and S. Shlomo, Nucl. Phys. **A608**, 32 (1996).
 - [17] A. A. Abrikosov and I. M. Khalatnikov, Rep. Prog. Phys. **22**, 329 (1959).
 - [18] V. M. Kolomietz, A. G. Magner and V. A. Plujko, Z. Phys. **A 345**, 131; 137 (1993).
 - [19] V. M. Kolomietz, V. A. Plujko and S. Shlomo, Phys. Rev. C **52**, 2480 (1995).
 - [20] H. S. Köhler, Nucl. Phys. **A378**, 159 (1982).
 - [21] J. Bartel, P. Quentin, M. Brack, C. Guet and H. -B. Hakansson, Nucl. Phys. **A386**, 79 (1982).

- [22] D. H. Youngblood, H. L. Clark and Y. W. Lui, Phys. Rev. Lett. **82**, 691 (1999).
- [23] A. Kolomietz, O. Pochivalov and S. Shlomo, Phys. Rev. C **61**, 034312 (2000).
- [24] D. H. Youngblood (private communication).

Figure captions

Fig. 1. The ratio $m_{02}(\xi)/m_1(\xi)$ of the partial contribution of the overtone to the EWSR as a function of the parameter ξ in the transition operator $\hat{f}_\xi(\mathbf{r})$ (Eq. (29)) obtained within the FLA (dashed line) and the HF-RPA (solid line) approaches, for the monopole mode $L = 0$ in the nucleus ^{208}Pb .

Fig. 2. The FLA and HF-RPA results for the fraction energy-weighted transition strength for the operator $\hat{f}_\xi(\mathbf{r})$ with $\xi = 78.6 \text{ MeVfm}^2$.

Fig. 3a. The HF-RPA transition density, $\tilde{\rho}_{\text{tr}}^{\text{HF-RPA}}(r)$, multiplied by $4\pi r^2$ for the overtone of the ISGMR in the nucleus ^{208}Pb (solid line) and the corresponding macroscopic transition density $\rho_{\text{tr}}^{\text{macr}}(\mathbf{r})$ taken at $\xi = 78.6 \text{ fm}^2$ (dotted line).

Fig. 3b. The FLA transition density, $\rho_{\text{tr}}^{\text{FLA}}(r)$, multiplied by $4\pi r^2$ for the overtone of the ISGMR in the nucleus ^{208}Pb (dashed line) and the corresponding macroscopic transition density $\rho_{\text{tr}}^{\text{macr}}(\mathbf{r})$ taken at $\xi = 68.3 \text{ fm}^2$ (dotted line).

Fig. 4. The ratio $m_{0n}(k)/m_1(k)$ for the main ($n = 1$) ISGMR and its overtone ($n = 2$), respectively, as a function of the wave number k obtained for electromagnetic operator $j_0(kr)Y_{00}(\hat{r})$ for the ^{208}Pb nucleus. The dashed and the solid lines represent the FLA and HF-RPA results, respectively.

Fig. 5. Partial contributions of the volume ("vol") and surface ("surf") terms of the FLA transition density of the ISGMR overtone (see Eq. (33)) to the integral in Eq. (50) (dashed lines). The solid line shows the sum of both the volume and the surface terms.

TABLE I: Comparison of the FLA and RPA results for the centroid energies (in MeV) for the main (E_{01}) and the overtone (E_{02}) modes of ISGMR. In the case of RPA calculations the values of E_{01} are obtained by integrating the strength function for the operator $r^2 Y_{00}$ over the energy range of 0 - 60 MeV and the values of E_{02} are obtained using the operator $(r^4 - \xi r^2) Y_{00}(\hat{\mathbf{r}})$ and the energy ranges of 35 - 60, 28 - 60, 27 - 55 and 25 - 50 MeV for ^{90}Zr , ^{116}Sn , ^{144}Sm and ^{208}Pb nuclei, respectively. The experimental data for the main tone is taken from the Ref. [22].

Nucleus	FLA			RPA			EXP.
	E_{01}	E_{02}	E_{02}/E_{01}	E_{01}	E_{02}	E_{02}/E_{01}	E_{01}
^{90}Zr	19.6	43.0	2.2	18.1	43.8	2.4	17.89 ± 0.20
^{116}Sn	18.2	40.4	2.2	16.5	39.1	2.4	16.07 ± 0.12
^{144}Sm	17.0	38.5	2.3	15.7	36.8	2.3	15.39 ± 0.28
^{208}Pb	15.3	35.5	2.3	13.8	33.7	2.4	14.17 ± 0.28

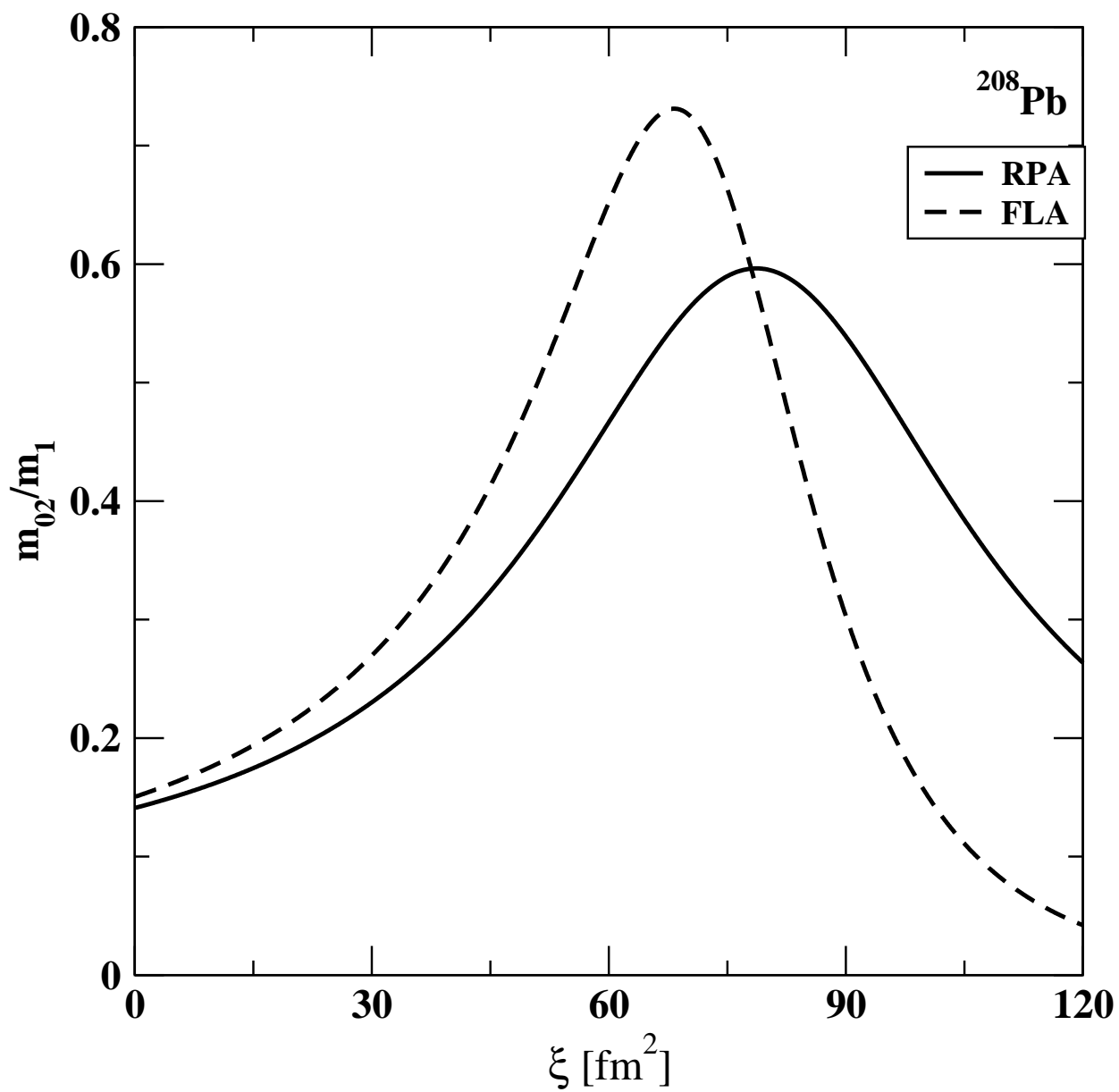


Fig.1

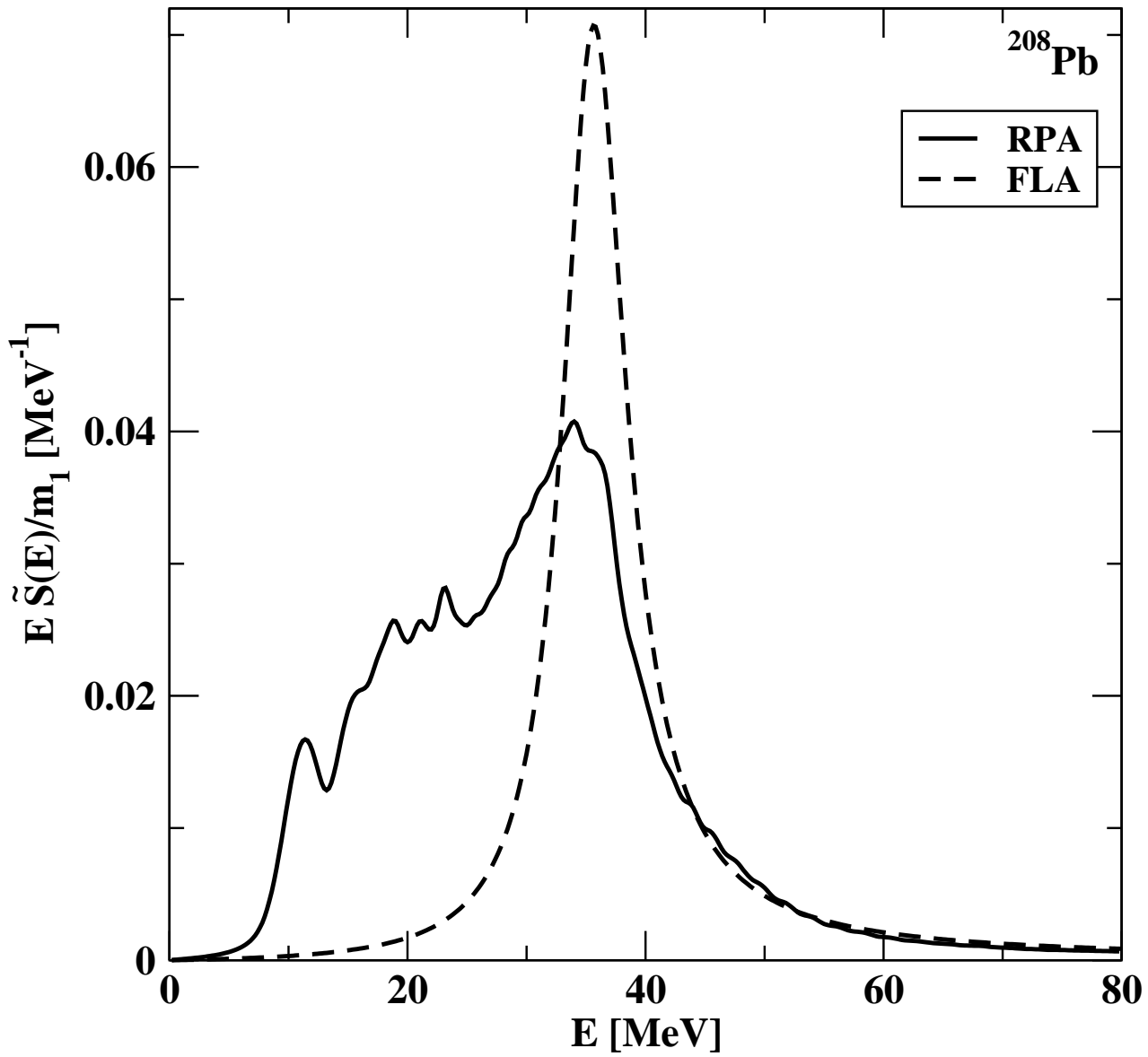


Fig. 2

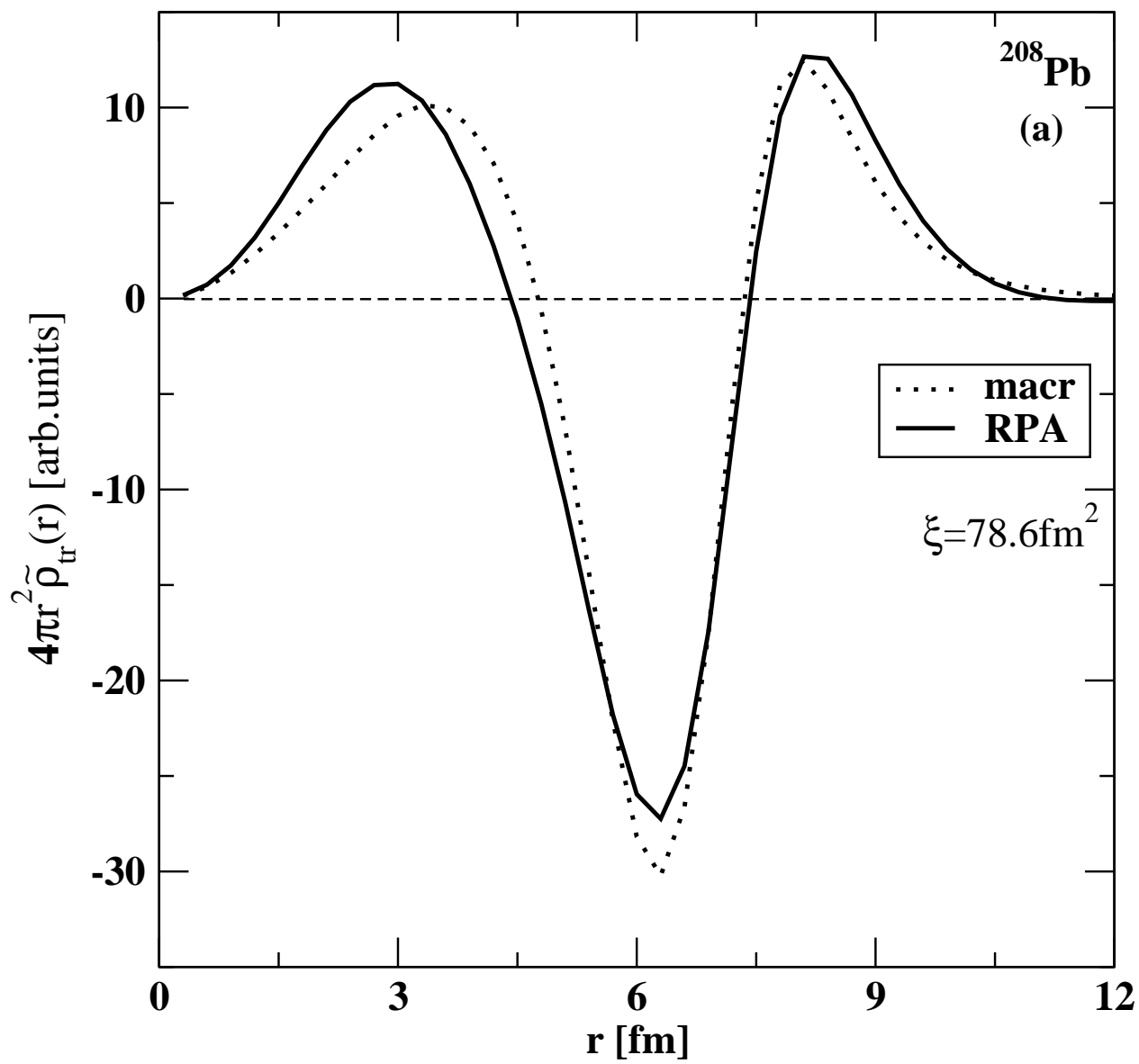


Fig. 3a

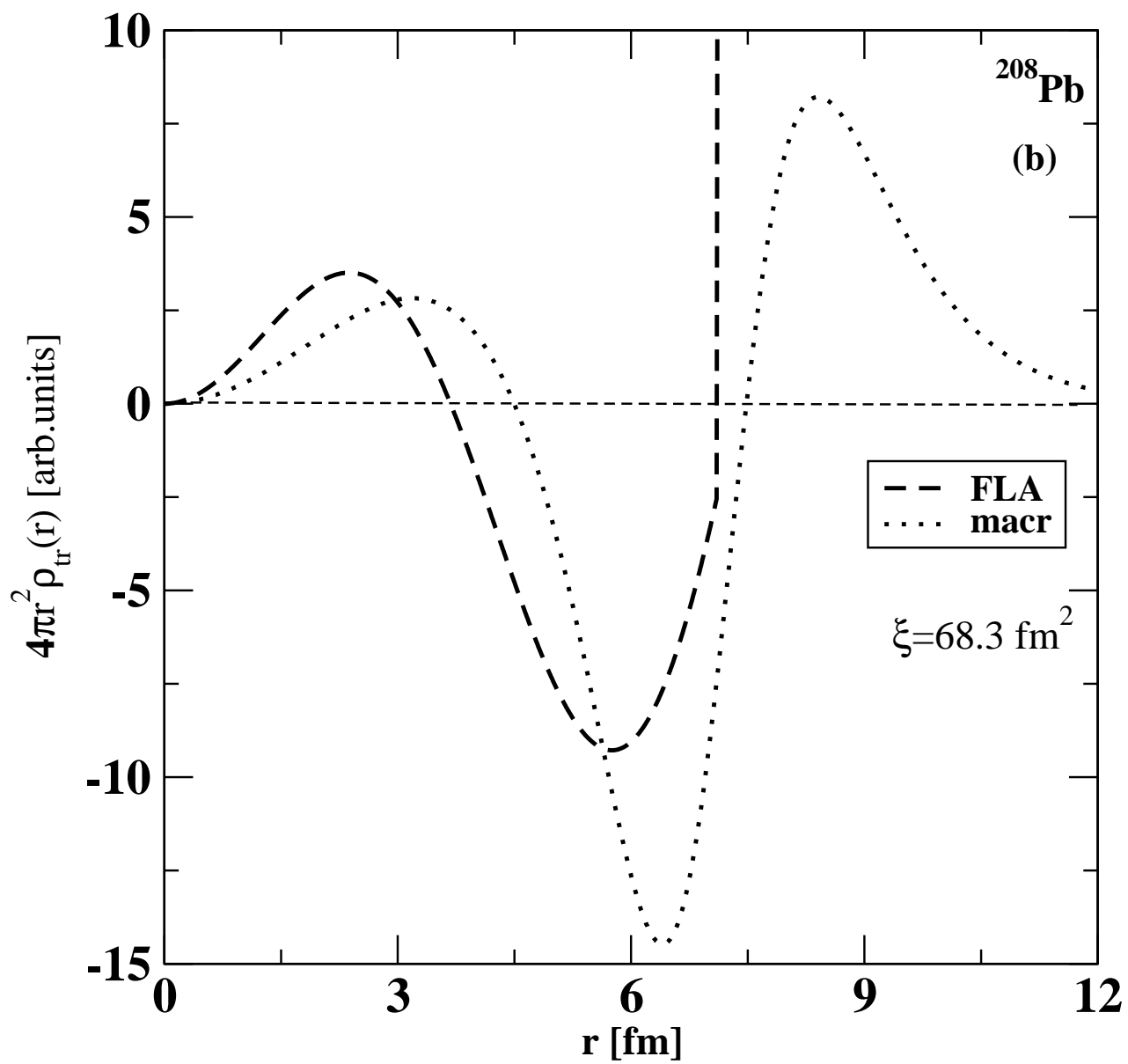


Fig. 3b

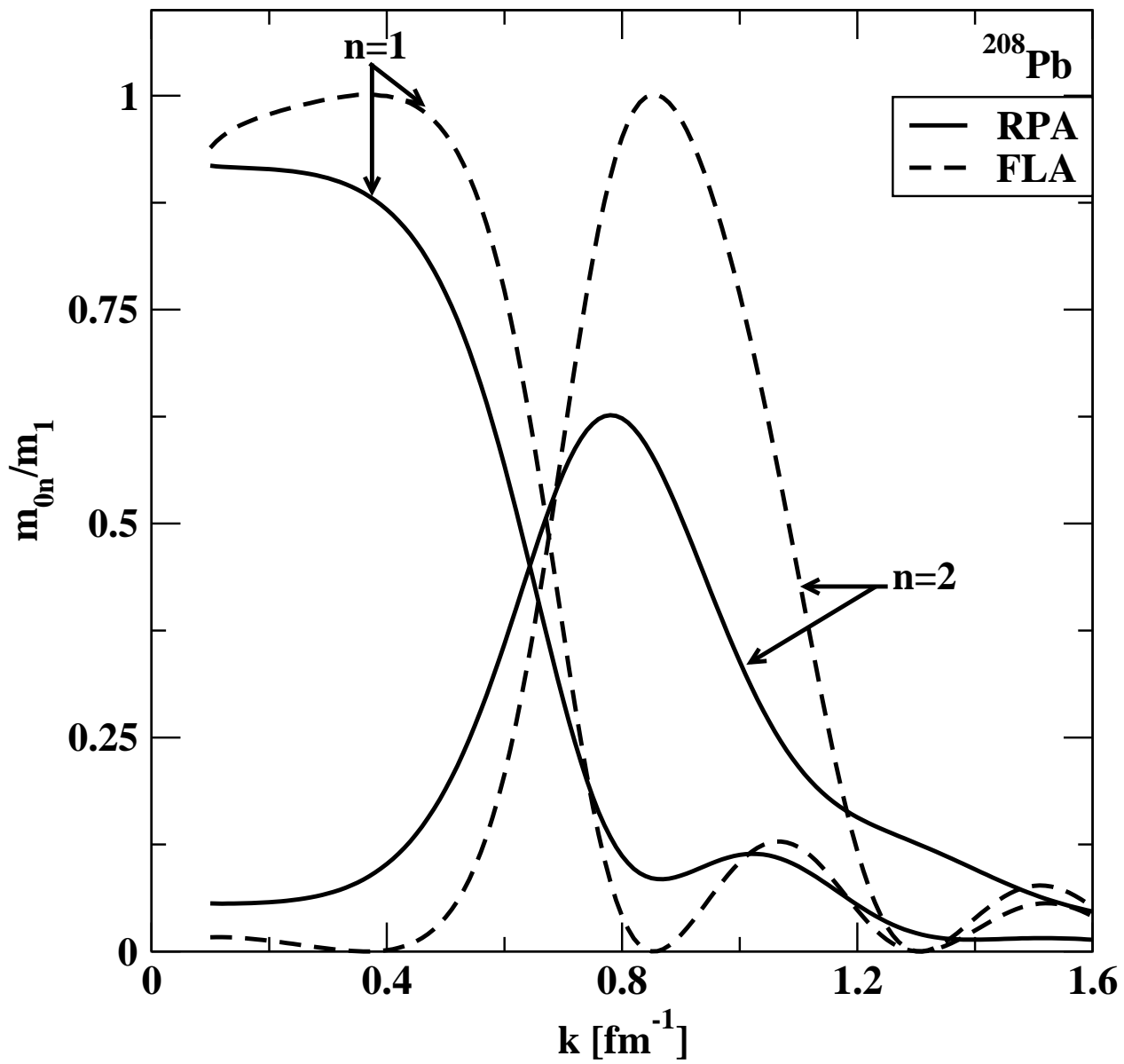


Fig. 4

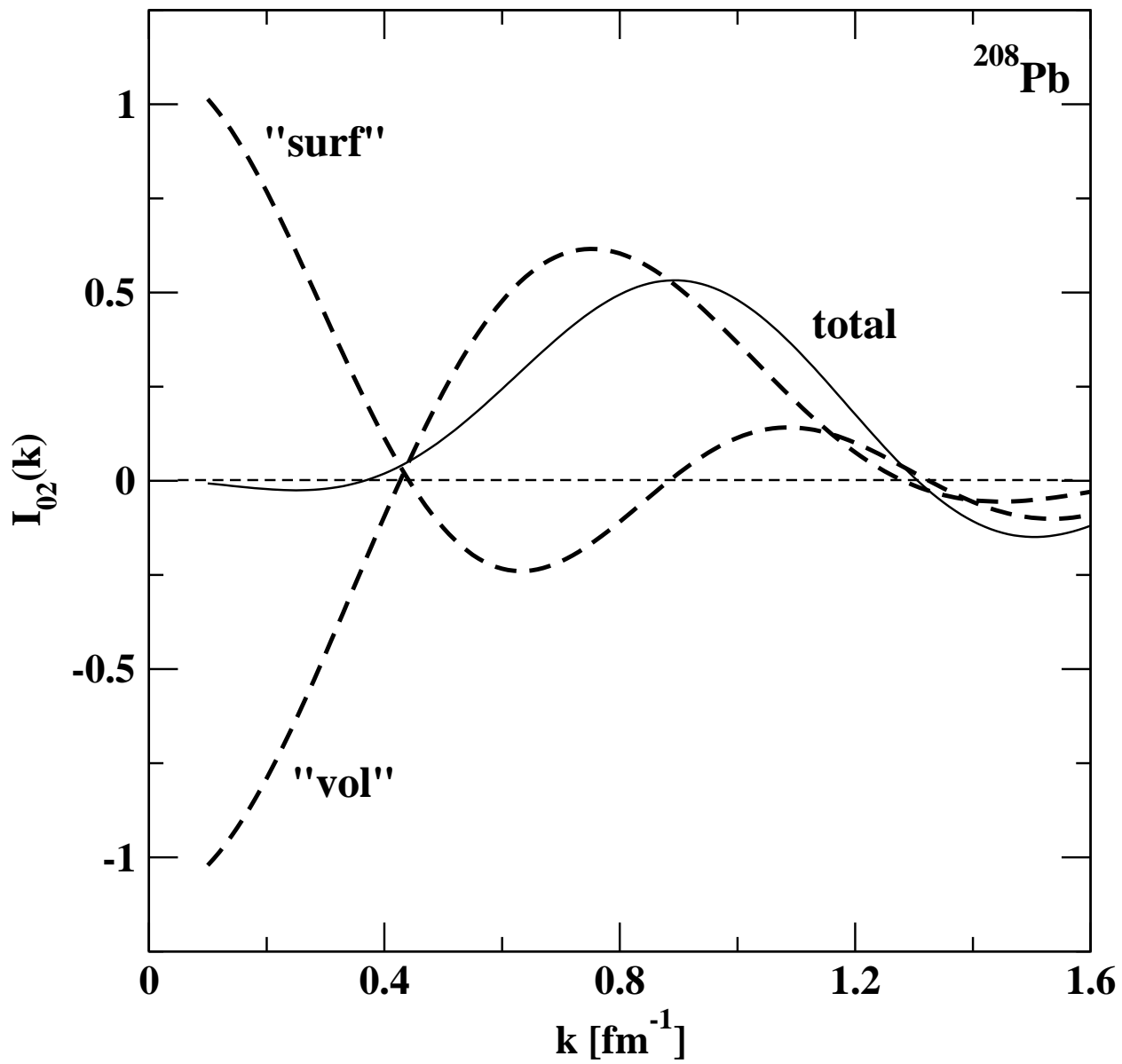


Fig. 5